2024 IEEE/ASME International Conference on Advanced Intelligent Mechatronics (AIM)
July 15-19, 2024. Boston, MA, USA

Metal Thickness Measurement Module with Scotch Yoke Mechanism for Tank Inspections

Yuki Nishimura
Zhejiang Lab
Hangzhou, China
nishimura.yuki.sg@alumni.tsukuba.ac.jp

Tao Zheng
Zhejiang Lab
Hangzhou, China
zhengtao2955@zhejianglab.com

Wei Song
Zhejiang Lab
Hangzhou, China
songwei_zju@163.com

***Abstract*—To avoid oil leakage accidents in large storage tanks, measurements of metal thicknesses are important to assess the structure conditions. Ultrasonic sensors are widely used to measure metal thicknesses. To realize ultrasonic thickness measurement by robots, it is necessary to realize contact between a probe and surfaces. In this study, we proposed a novel mechanism of a metal thickness measurement module which includes a Scotch Yoke mechanism to convert a robot's movement to a pressing motion of a probe. The proposed module consists of a probe, a slider box, a slider, wheels, and a rotation disk with a pin. When the disk connected to the wheels rotates, the pin moves the slider connected to the probe up and down simultaneously. The module mounted on a magnet-type wall-climbing robot measured the metal thicknesses of the test pieces. We confirmed that the prototype module can realize the contacting and releasing of the probe to surfaces according to the wheel's rotation.**

Keywords—Tank inspection, ultrasonic, thickness measurement, wall-climbing robot.

I. INTRODUCTION

Oil leakage accidents happen when oil tanks are ruptured. To avoid those accidents, tanks are recommended to be totally scanned by ultra-sonic sensors [1]. In China, there are 7,000 oil storage tanks and the largest volume of tanks is 15,000 m^3 [2]. Current structure inspection relies on human inspection which requires a considerable amount of cost, time, and labor [3]. Moreover, workers are at risk from climbing large structures, entering closed spaces, and exposure to chemical contaminants. Therefore, autonomous robots which carry out tank inspection and maintenance have been proposed. Wall-climbing robots can replace humans in the inspection of large storage tanks because they can improve work efficiency, save the cost of building scaffolds, and eliminate the danger of manual work [4]. For example, a weld seam tracking and image inspection by a magnet-type wheeled robot has been proposed [5, 6]. In addition, metal thickness measurements by ultrasonic sensors are also common for Non-Destructive Testing (NDT). Therefore, wall-climbing robots with permanent magnet adhesion mechanisms were proposed to carry ultrasonic sensors for inspections [7, 8]. Also, a climbing robot with a vacuum suction module was developed to carry sensors for NDT on vertical surfaces [9].

However, actual thickness measurement with mounted ultrasonic sensors was not tested in these studies. One of the reasons that studies on thickness measurement by robots are limited is the difficulty of a procedure of ultrasonic thickness measurement. Ultrasonic thickness measurements require the probe (transducer) to make contact with a target surface with an appropriate force to ensure adequate coupling of the transmitted acoustic energy [10]. To realize this procedure, an electric putter attached to a climbing robot to actuate a probe [11], an arm realized a gentle touch of a probe to steel surfaces [12], and a four-bar mechanism to realize probe movements [13] have been proposed for autonomous thickness measurement. These measurement methods use actuators to make contacts, the system will be complex and its weight will increase despite that climbing robots have strict limitations on payloads.

The impact of unmanned aerial vehicles (UAVs) has been increased in monitoring and inspection tasks [14]. A UAV with an ultrasonic probe can approach any place of the structure by flying and sticking to the target place [15]. In [10], a probe attached to a spring-loaded arm extending from a UAV was guided and undertook a contact thickness measurement process without manual intervention. In [16], a UAV conducted ultrasonic thickness measurements by flying, approaching, and contacting a surface with a sensor. Other than using regular probes, a dry-coupled ultrasonic wheel probe was deployed to a UAV [17]. This UAV can fly to target surfaces, press the probe to surfaces, and obtain thickness. UAVs with probe-attached arms are simple; however, navigation to target points is difficult and measurement resolution is not high. In addition, the time duration of operation is limited compared to climbing robots.

Although many approaches have been made, the solid method has not been realized for ultrasonic thickness measurements by climbing robots. Existing inspection robots need to move a measurement point, stop at the point, touch a surface with a probe with actuators, measure the thickness, and then move again. In the case of UAVs, they need to fly close to surfaces and fly away from surfaces repeatedly to measure a target area. In this study, we proposed a novel ultrasonic metal thickness measurement module for tank inspection by climbing robots. The proposed module realizes a probe contact just with the movements of a robot without additional actuators. It can contact the surface at the same interval continuously. The proposed mechanism is simple but can be used in various types of contact inspection (e.g. coating thickness measurements). The originality is that the stroke motion for an ultrasonic probe is realized by the Scotch Yoke mechanism which converts the wheel rotation to the stroke motion.

This work was supported by the "Pioneer" and "Leading Goose" R&D Program of Zhejiang (2023C03186).

The structure of this manuscript is as follows. In Section II, we explained the basic principle of ultrasonic thickness measurement and proposed the measurement module that uses the Scotch Yoke mechanism. In Section III, the prototype proposed module is developed. We conduct experiments to confirm the ability of thickness measurement by the module in Section IV. Its results and limitations of the proposed module are discussed in Section V. Finally, the conclusion is shown in Section VI.

II. Thickness Measurement Mechanism

A. Ultrasonic Thickness Measurement

In metal thickness measurements, a probe needs to be in contact with a surface of a target object, then, an ultrasonic wave is emitted from the contact point between the probe and the surface (see Fig. 1). The ultrasonic wave is reflected on the opposite surface of the object and then returns to the probe again. The thickness is calculated from the relationship between the propagation time and the sound speed inside the object being measured. The common method to calculate metal thickness with an ultrasonic thickness gauge is written as

$$H = \frac{vt}{2} \tag{1}$$

where H is metal thickness, v is sound velocity inside the material, and t is the round-trip transit time of sound. A manual measurement requires the worker to push the probe to surfaces over and over again. To automate thickness measurements by robots, this pressing motion of the probe to make contact with surfaces needs to be generated mechanically.

B. Scotch Yoke Mechanism

Many mechanisms have been developed to produce a linear motion from a rotary motion to be utilized in many applications [18]. The Scotch Yoke mechanism is also designed to convert the rotational motion to linear motion [19]. This mechanism is widely used in robot systems such as a quadruped robot insect [20], a needle insertion robot [21], and a dolphin-like robot [22].

Fig. 2 illustrates a schematic diagram of the conventional Scotch Yoke mechanism [19, 22–25]. The pin of the rotation disk is contacting the slider at P where θ is the rotating angle of the disk. L_1 is the length between the pin and the rotation disk center O. L_2 is the length of the arm between the slider and the end effector Q. The coordinates of point P are written as

$$\begin{cases} x_P = L_1 \cos\theta \\ y_P = L_1 \sin\theta \end{cases} \tag{2}$$

where x_P and y_P are the x and y coordinates of P, respectively. Therefore, the horizontal movement of Q is written as

$$x_Q = L_1 \cos\theta + L_2 \tag{3}$$

where x_Q is the x coordinate of Q. The end effector reaches its maximum length when θ is 0°. And then, when θ is 180°, the end effector reaches its minimum.

In this study, we use the Scotch Yoke mechanism to generate a pressing motion of a probe for ultrasonic thickness measurements. Because the climbing movement of a robot is converted to the pressing motion of the probe, the robot does not need additional actuators, control boards, and batteries.

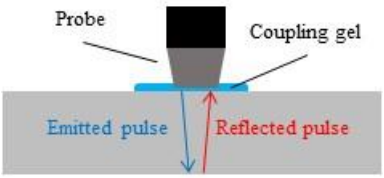

Fig. 1. Basic principle of ultrasonic thickness measurement.

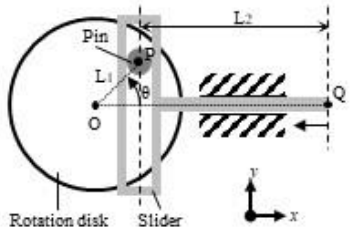

Fig. 2. Schematic diagram of Scotch Yoke mechanism.

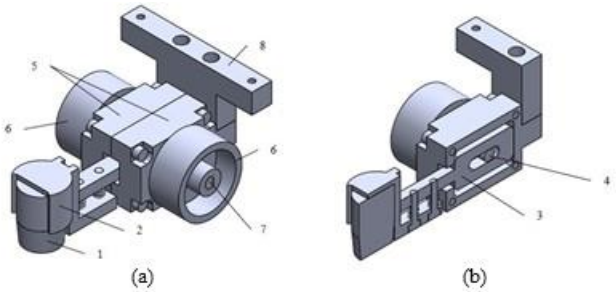

Fig. 3. Proposed measurement module. (a) Overview, (b) cutway view.

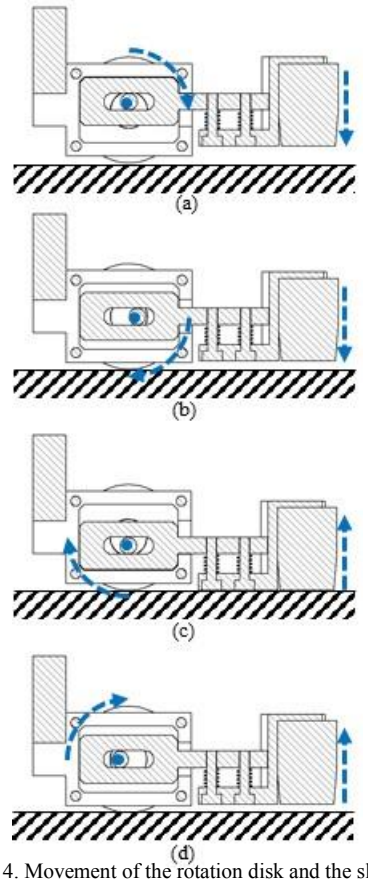

Fig. 4. Movement of the rotation disk and the slider.

C. Proposed Design of Metal Thickness Measurement Module

Fig. 3(a) and (b) show an overview of the proposed module and its inside structure, respectively. The measurement module consists of eight parts; (1) a probe, (2) a probe holder, (3) a slider, (4) a rotation disk with a pin, (5) a slider box, (6) wheels, (7) wheel shafts, and (8) an attachment part. The rotation disk is connected to the wheel with the shaft. Therefore, the rotation disk rotates according to the robot's movement. When the rotation disk with a pin rotates, the pin makes the slider move up and down. The probe is connected to the slider. So, the probe can touch the surface. The springs are used to absorb the surface's roughness and support the probe to touch the surface properly.

Figs. 4(a) to (d) show mechanical diagrams of the proposed module. Single contact motion to the surface is divided into four phases. In phase 1, the slider with a probe is located at the upper limit. This is achieved when the pin of the rotation disk is at the top, the slider is lifted upwards until maximum limitation (see Fig. 4(a)). In phase 2, when the rotation disk rotates according to the wheels' rotation, the pin of the rotation disk pushes down the slider and the probe. Then, the probe approaches the ground (see Fig. 4(b)). In phase 3, when the pin of the rotation disk is at the bottom, the slider is pushed down to the lower limit. At this point, the probe touches the surface (see Fig. 4(c)). In phase 4, the pin moves upwards and the slider is lifted upward until it reaches the maximum limitation (see Fig. 4(d)). By repeating this, the proposed module provides periodic contacts of the probe to the surface from the running wheels of the robot.

D. Proposed Situation of Using the Module

With its feature of simplicity and being required no actuators, the module can be used in different forms. In [26], a proposed impact mechanism for hammering inspection was tested in three different conditions where the mechanism was attached to: the end of a rod and moved manually, an arm that was installed on an Unmanned Ground Vehicle (UGV), and a climbing robot. In the same way, the proposed module can be used in various conditions as listed below:

Handle: A handle is simply attached to the module. The module is moved manually to measure thickness.

Rod: It is similar to handles but the module is attached to one end of a rod. With the rod, the module can reach higher places.

UGV with robot arm: A robot arm with the module can contact a surface. Measurements can be automated with a UGV but a measurement area is limited to the robot arm movement range.

Climbing robot: The module can be installed on a climbing robot which can move freely on walls. This lightweight module can be mounted even if the robot has payload limitations.

UAV: The module can be attached to an arm of a UAV. Once the module contacts a surface, the UAV only needs to fly up or down while keeping the module in contact. There is no need to fly close to the surface and fly away from the surface repeatedly.

The proposed metal thickness measurement module is intended to be used in a variety of situations. In this study, we conducted experiments and verified the handle-installed, rod-installed, and climbing-robot-installed situations using the same module. However, the design can be changed flexibly to suit each environment and allow more efficient measurements.

Fig. 5. Developed module. (a) Overview, (b) side view.

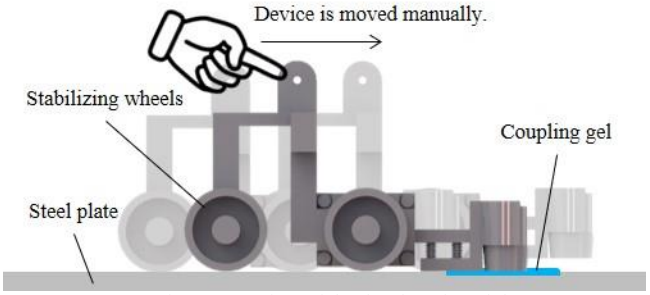

Fig. 6. Overview of the developed module.

III. Development of Device

Based on the design in Section II, we developed a prototype of the measurement module as shown in Figs. 5(a) and (b). The size of the module was 46 mm in height, 66 mm in width, and 92 mm in length. The module weight was 84 g and the probe weight was 43 g. The wheel diameter was 32 mm which was designed to contact the surface in 100 mm intervals (pitches). The measurement interval distance d was calculated as

$$d = 2\pi r \tag{4}$$

where r is a wheel radius. The interval distance can be designed according to the requirements of the task by simply modifying the wheel diameter. The module parts were 3D printed with ABS-like SL resin (C-UV 9400). To increase the friction coefficient between steel surfaces and 3D-printed wheels, we attached an anti-slip tape on wheels. The probe of the ultrasonic sensor was attached to the probe holder. We used a commercially available probe and ultrasonic thickness gauge (SW-6510S by SNDWAY) and its weight was 180 g.

IV. Experiments and Results

To evaluate the validity of the developed module, we conducted three experiments of metal thickness measurements on the actual metal surfaces. First, we measured metal thicknesses with the developed module by hand, then installed the module to the measurement rod and measured the steel pillar thickness. Finally, we installed the module to the wall-climbing robot and showed ability as metal thickness measurement equipment for inspection by climbing robots.

A. Fundamental Metal Thickness Measurement Experiment

First, we prepared two types of metal plates for testing. The ground truth thicknesses of test metal plate 1 and 2 by the thickness gauge were 5.76 mm and 3.68 mm, respectively. The

measured thickness by the module has a mechanical offset. Therefore, this offset was subtracted from Eq. (1) as

$$H = \frac{vt}{2} - H_{offset} \quad (5)$$

where H_{offset} (= 0.40 mm) is the offset obtained in the fundamental experiment. In the rest of the papers, we use this offset to calculate the thickness of the metal plate.

The experimental setting is shown in Fig. 6. We attached stabilizing wheels to the module so that the wheels of the module can be rolled on metal plates. To compare the manual-measured and module-measured thickness of the test pieces, we moved the module straight on the test pieces, confirmed the probe contacted surfaces when wheels rotated on surfaces, and read the thickness of the gauge. Coupling gel was dispensed on measurement points in advance. We performed 50 measurements for each test piece.

Fig. 7 shows measurement results with error bars from the experiment. The average of module-measured thicknesses of the test plate 1 and 2 were 5.77 mm and 3.66 mm, respectively. Standard deviations of manual measurements were 0.02 in Test 1 and 0.04 in Test 2 while standard deviations of module measurements were 0.30 in Test 1 and 0.21 in Test 2.

B. Experiment with Measurement Rod

To simulate the usage situation listed in Section III-C, we attached the developed module to a measurement rod and conducted an experiment to measure the thickness of an actual structure (see Fig. 9). The rod was made of 10 mm squared Aluminum pipes where the module was installed on one end and the digital thickness gauge was installed on another end. The experiment was conducted on the I-beam (H-shaped) steel pillar of our laboratory. Based on Otsuki *et al.* [13], we measured at 12 points (see Fig. 9(a)). The distance of each point was 100 mm. Coupling gel was dispensed on these 12 points in advance.

The measurement results were displayed as a color map in Fig. 9(c). As reference ground truth, thicknesses measured manually were also displayed as a color map in Fig. 9(b). Thicknesses between two neighboring measurement points are linearly interpolated in color maps. The average measured thickness by the module was 6.96 mm and its reference value was 6.94 mm. Moreover, the two color maps share the same tendency that measured thicknesses are thickest at A4, and thinnest at B2.

C. Experiment with Wall-Climbing Robot

To show the ability of thickness measurement by robots with the proposed module, we installed the developed module on a climbing robot. Because our inspection target object is large storage tanks made with ferromagnetic materials, we used a magnet-type wall-climbing robot for the experiment. The magnet-type wall-climbing robot can show steady movement on steel objects [27] because suction-type robots have a limitation on surface roughness [9] and propeller-type robots have a limitation on operation time [28,29]. Therefore, magnet-type robots are widely used for steel-made tank inspection [5–8].

A magnet-type wall-climbing robot used in this study was designed to carry a total of 9 kg including 3.2 kg of the robot

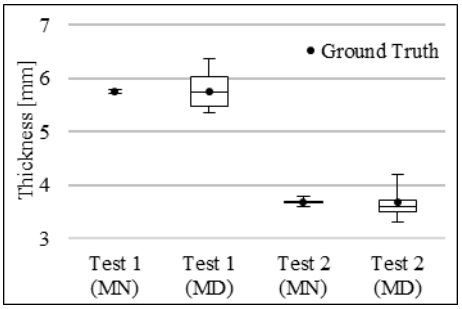

Fig. 7. Measurement results (MN: manual, MD: module).

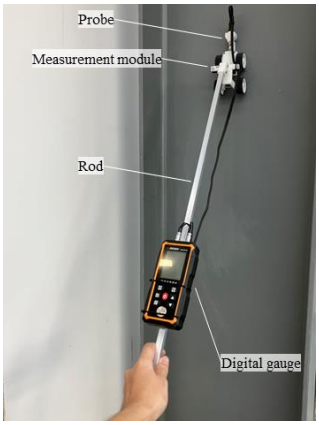

Fig. 8. Measurement module with the rod.

itself weight and 0.6 kg of a 6000 mAh LiPo battery. The required magnetic adhesion force is 620 N because the friction coefficient of a metal surface was 0.22 when the safety factor was 1.5. The developed robot has three wheels, two of them are magnet wheels [30], and one is free rotating non-magnet wheel (see Figs. 10(a) and (b)). The magnetic wheel (44 mm in diameter, 26 mm in width, and 0.35 kg in weight) has an adhesion force of 250 N. The plate magnet (75 mm in width and length, 25 mm in height, and 1.05 kg in weight) on the robot body has an adhesion force of 120 N. The robot (275 mm x 260 mm x 100 mm) uses a geared brushless DC motor (JGB37-3650) for propulsion. It can reach a maximum speed of 18.7 m/min and clear obstacles up to 4 mm high. The robot and its controller, are both equipped with Arduino UNO and a Wi-Fi module.

As shown in Fig. 11, the module was attached in front of the robot, and the digital gauge was attached to the main body. The metal thickness measurement experiment was conducted on the steel pillar shown in Fig. 9(a). In this experiment, the robot with the module was controlled to move straight from B1 to B4 where the points that coupling gel was dispensed in advance. The robot was controlled manually by the controller. We observed that the wheels of the module rotated according to the robot's movement and then the probe contacted the surface. The measured thickness and the actual thickness are shown in Fig. 12. The reference, rod-measured, and robot-measured average thickness of B1 to B4 were 6.89 mm, 6.84 mm, and 5.90 mm, respectively.

V. DISCUSSION

Through experiments, we observed that the developed metal thickness measurement module functioned as expected. The wheels of the module rotated according to the robot's movement and the probe contacted the surface to measure thickness by the

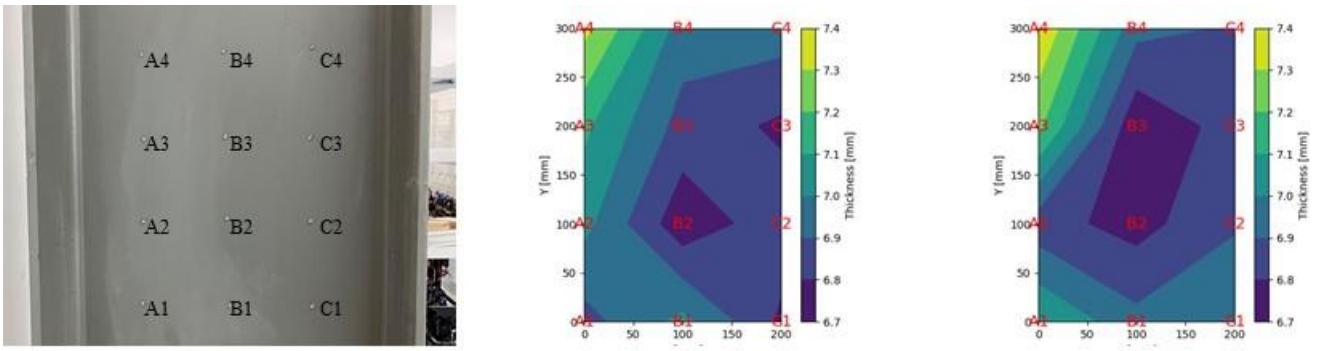

(a) (b) (c)

Fig. 9. Measurement experiment on a steel pillar. (a) Steel pillar with measured points, (b) color map of reference thickness, (c) measured thickness.

ultrasonic thickness gauge. Also, we showed that this module can be used in many ways such as being moved manually (see Fig. 6), with the measurement rod to measure the surface in high places (see Fig. 8), and with the robot (see Fig. 11). The module can efficiently inspect a wider area with constant intervals.

The reference and module-measured thicknesses were compared. The average thickness was 5.76 mm for reference and 5.77 mm in Test 1. The average thickness was 3.68 mm for reference and 3.66 mm in Test 2. The errors were +0.17% for Test 1 and -0.54% for Test 2. However, this experiment revealed that the module has large standard deviations compared with manual measurements. The gaps between moving parts, necessary for the smooth movement of the shaft and slider, may affect the measurement accuracy and cause a large standard deviation when using the module. reference and rod-measured thickness had a +0.29% error in average thickness of 12 points and showed the same tendency in color maps. Therefore, we mounted the module on the robot and confirmed that the module was able to move its probe according to the robot's movement on the steel pillar. Although, we measured only B1 to B4, the error between reference and robot-measured thickness is larger than using the measurement rod.

There are several possible reasons for these errors. First, the offset value may be different when pressing by hand and by the robot. The offset was measured manually in Section IV-A; however, it's essential to examine the offset resulting from the actual robot's movement on a test structure for more accurate results. Second, we observed a problem with the controlling of the robot. During experiments, the probe was not properly grounded on the measurement points due to the robot's movement error on the steel surface. The driving wheels of the robot were controlled by switching them ON and OFF. Therefore, vibrations occurred when the robot started moving and when it stopped, and this vibration affected the contact of the probe to surfaces. To reduce vibrations, it is desirable to use a control method such as the S-curve control [31]. Also, the amount of time to press the probe depends on the speed of the running wheels. It should be considered how the pressing force changes depending on the robot's speed. In addition, the probe holder with spring should be improved to press the probe with a more constant angle to surfaces.

A. Limitation

In ultrasonic metal thickness measurements, robots need to properly dispense coupling agents and firmly press a probe on

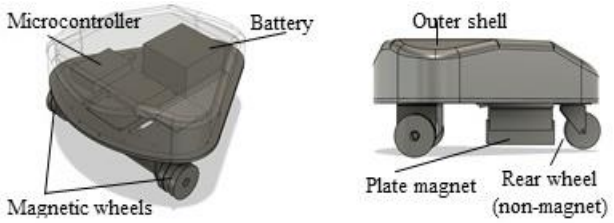

(a) (b)

Fig. 10. Design of the wall-climbing robot. (a) Overview, (b) side view.

Fig. 11. Robot with the measurement module.

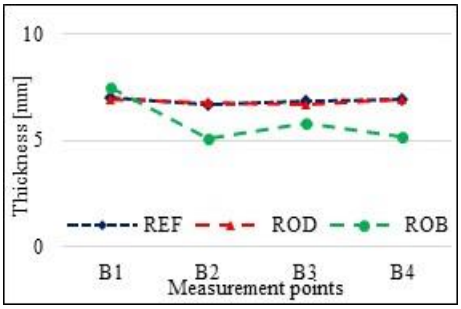

Fig. 12. Robot with the measurement module (REF: reference, ROD: rod-measured, ROB: robot-measured thickness).

measurement surfaces [13]. A coupling agent must be placed between the target surface and the probe to eliminate any air gaps [10]. However, the dispensing of coupling gel is not discussed in this manuscript. In experiments in Section IV, coupling gel was manually dispensed. A UAV with an ultrasonic measurement gauge can realize only four measurements by a single dose because of the limitation of coupling gel [16]. Otsuki *et al.* equipped a pumping mechanism for their robot for dispensing coupling gel [13]. Their pumping mechanism can carry coupling gel for 30 measurements. Therefore, Mattar *et al.* attached an elastomer as a dry coupling to the probe of their

UAV system [15]. Dry couplings eliminate the need for the application of any liquid couplings and the inconvenience associated with it [32]. It is necessary to develop a mechanism that automatically dispenses coupling gel as well as moves a probe to surfaces. Also, we need to consider the use of dry couplings to eliminate the need for dispensing coupling gel for continuous measurement without any refills of coupling gel.

VI. Conclusion

In large storage tank inspections, the metal thickness of the tank is measured for their assessments. In this study, we introduced a method to make the metal thickness measurement more efficient. The ultrasonic thickness gauge normally requires its probe to be repeatedly grounded and separated from the target surface during measurements. Therefore, we proposed and developed the module using the Scotch Yoke mechanism to push the ultrasonic probe to surfaces automatically. The Scotch Yoke mechanism can convert the rotation movement of wheels when a robot climbs surfaces to the pressing motion of the probe without additional actuators. We conducted basic measurement experiments on an actual steel pillar using a magnet-type wall-climbing robot with the developed module. From the experiment results, we confirmed that the developed module was able to rotate its wheels and move the probe up and down in response to the movement of the robot.

By contrast, the problem of coupling agents needs to be addressed in future work. Proper use of coupling gel ensures the probe is in close contact with the target surface, allowing for accurate thickness measurements. In addition, the actual tank surface is curved and has irregularities such as welded seams. Therefore, we need to operate and test the robot with the module on the surfaces of actual tanks.

References

[1] "Safety alert: Rupture of an (atmospheric) crude oil storage tank - Belgium," Chemical Risks Division, emploi.belgique.be, 2006. https://emploi.belgique.be/sites/default/files/content/documents/The%20well-being%20of%20workers/Seveso/ONG013-E-v1.pdf (accessed Jan. 3, 2024).

[2] "Chang ya chu guan an quan jian ce fa zhan qu shi," General Administration of Quality Supervision, Inspection and Quarantine of PR China, 2014. http://www.chinatt315.org.cn/zljd/2014-1/3/141130.html (accessed Jan. 3, 2024).

[3] Y. Otsuki *et al.*, "Ultrasonic thickness measurement using the martlet wireless sensing system," *IEEE I2MTC*, 2021. DOI: 10.1109/I2MTC50364.2021.9460094.

[4] W. Zhang *et al.*, "Localization of wall climbing robot on cylinder-shaped steel," *Adv. in Transdisciplinary Eng.*, 2022. DOI: 10.3233/atde221179.

[5] J. Li *et al.*, "Weld seam identification and tracking of inspection robot based on deep learning network," *Drones*, 2022, DOI: 10.3390/drones6080216.

[6] J. Li *et al.*, "Spatial positioning robotic system for autonomous inspection of LPG tanks," *Industrial Robot: Int. J. Robotics Res. and App.*, 2022. DOI: 10.1108/ir-03-2022-0076.

[7] L. P. Kalra *et al.*, "A wall climbing robot for oil tank inspection," *IEEE ROBIO*, 2006. DOI: 10.1109/ROBIO.2006.340155.

[8] W. A. Blyth *et al.*, "A reduced actuation Mecanum wheel platform for pipe inspection," *IEEE AIM*, 2016. DOI: 10.1109/AIM.2016.7576803.

[9] J. Xiao *et al.*, "Rise-rover: A wall-climbing robot with high reliability and load-carrying capacity," *IEEE ROBIO*, 2015. DOI: 10.1109/ROBIO.2015.7419079.

[10] D. Zhang *et al.*, "Autonomous ultrasonic inspection using unmanned aerial vehicle," *IEEE IUS*, 2018. DOI: 10.1109/ULTSYM.2018.8579727.

[11] Y. Ding *et al.*, "Non-contacted permanent magnetic absorbed wall-climbing robot for ultrasonic weld inspection of spherical tank," *MATEC Web Conf.*, 2019. DOI: 10.1051/matecconf/201926902013.

[12] M. Phlernjai and P. Ratsamee, "Multi-legged inspection robot with twist-based crouching and fine adjustment mechanism," *J. Robotics Mechatronics*, 2022. DOI: 10.20965/jrm.2022.p0588.

[13] Y. Otsuki *et al.*, "Autonomous ultrasonic thickness measurement of steel bridge members using a climbing bicycle robot," *J. Eng. Mechanics*, 2023. DOI: 10.1061/jenmdt.emeng-7000.

[14] M. Martynov *et al.*, "Morphogear: An UAV with multi-limb morphogenetic gear for rough-terrain locomotion," *IEEE AIM*, 2023. DOI: 10.1109/AIM46323.2023.10196115.

[15] R. A. Mattar and R. Kalai, "Development of a wall-sticking drone for non-destructive ultrasonic and corrosion testing," *Drones*, 2018. DOI: 10.3390/drones2010008.

[16] L. M. González-deSantos *et al.*, "Payload for contact inspection tasks with UAV systems," *Sensors*, 2019. DOI: 10.3390/s19173752.

[17] R. Watson *et al.*, "Dry coupled ultrasonic non-destructive evaluation using an over-actuated unmanned aerial vehicle," *IEEE T-ASE*, 2022. DOI: 10.1109/TASE.2021.3094966.

[18] H. A. Hussain, "A novel contactless rotary-to-linear magnetic actuator," *IEEE IEMDC*, 2019. DOI: 10.1109/IEMDC.2019.8785222.

[19] Y. Pu *et al.*, "A novel linear switch reluctance generator system," *IEEE ICAL*, 2012. DOI:10.1109/ICAL.2012.6308245.

[20] L. Liao *et al.*, "Design and implementation of a quadruped robot insect," *IEEE ICMA*, 2015. DOI:10.1109/ICMA.2015.7237495.

[21] Y. Qiu *et al.*, "Mri-compatible hydraulic drive needle insertion robot," *IEEE ICARM*, 2021. DOI: 10.1109/ICARM52023.2021.9536120.

[22] J. Yu *et al.*, "An adjustable scotch yoke mechanism for robotic dolphin," *IEEE ROBIO*, 2007. DOI:10.1109/ROBIO.2007.4522215.

[23] V. Arakelian *et al.*, "Design of scotch yoke mechanisms with improved driving dynamics," *Proc. Institution of Mech. Eng., Part K: J. Multi-body Dynamics*, 2015. DOI: 10.1177/1464419315614431.

[24] D. Chung *et al.*, "Gravity compensation mechanism for roll-pitch rotation of a robotic arm," *IEEE IROS*, 2016. DOI: 10.1109/IROS.2016.7759076.

[25] A. Al-Hamood *et al.*, "Dynamics and lubrication analyses of scotch yoke mechanism," *IJIDeM*, 2019. DOI: 10.1007/s12008-019-00545-y.

[26] T. Yamaguchi *et al.*, "Hammering robot for concrete surface inspection," *IASTED Int. Conf. on Robotics*, 2011. DOI: 10.2316/p.2011.752-064.

[27] W. Song *et al.*, "A path tracking method of a wall-climbing robot towards autonomous inspection of steel box girder," *Machines*, 2022. DOI: 10.3390/machines10040256.

[28] Y. Nishimura and T. Yamaguchi, "Development of a steep slope mobile robot with propulsion adhesion," *IEEE IROS*, 2020. DOI: 10.1109/IROS45743.2020.9341524.

[29] Y. Nishimura *et al.*, "Automated hammering inspection system with multi-copter type mobile robot for concrete structures," *IEEE RAL*, 2022. DOI: 10.1109/LRA.2022.3191246.

[30] W. Song *et al.*, "Design of permanent magnetic wheel-type adhesion-locomotion system for water-jetting wall-climbing robot," *Adv. Mech. Eng.*, 2018. DOI: 10.1177/1687814018787378.

[31] P. Meckl and P. Arestides, "Optimized s-curve motion profiles for minimum residual vibration," *Proc. ACC*, 1998. DOI: 10.1109/ACC.1998.688324.

[32] A. Allam *et al.*, "Detachable dry-coupled ultra-sonic power transfer through metallic enclosures," *IEEE IUS*, 2021. DOI: 10.1109/IUS52206.2021.9593569.